Development 127, 1833-1843 (2000)
Printed in Great Britain © The Company of Biologists Limited 2000
DEV4303

Temporal and spatial gradients of *Fgf8* and *Fgf17* regulate proliferation and differentiation of midline cerebellar structures

Jingsong Xu, Zhonghao Liu and David M. Ornitz*

Department of Molecular Biology and Pharmacology, Washington University School of Medicine, St Louis, MO 63110, USA
*Author for correspondence (e-mail: dornitz@molecool.wustl.edu)

Accepted 31 January; published on WWW 6 April 2000

SUMMARY

The midbrain-hindbrain (MHB) junction has the properties of an organizer that patterns the MHB region early in vertebrate development. *Fgf8* is thought to mediate this organizer function. In addition to *Fgf8*, *Fgf17* and *Fgf18* are also expressed in the MHB junction. *Fgf17* is expressed later and broader than either *Fgf8* or *Fgf18*. Disrupting the *Fgf17* gene in the mouse decreased precursor cell proliferation in the medial cerebellar (vermis) anlage after E11.5. Loss of an additional copy of *Fgf8* enhanced the phenotype and accelerated its onset, demonstrating that both molecules cooperate to regulate the size of the precursor pool of cells that develop into the cerebellar vermis. However, expression patterns of *Wnt1*, *En2*, *Pax5* and *Otx2* were not altered suggesting that specification and patterning of MHB tissue was not perturbed and that these FGFs are not required to pattern the vermis at this stage of development. The consequence of this developmental defect is a progressive, dose-dependent loss of the most anterior lobe of the vermis in mice lacking *Fgf17* and in mice lacking *Fgf17* and one copy of *Fgf8*. Significantly, the differentiation of anterior vermis neuroepithelium was shifted rostrally and medially demonstrating that FGF also regulates the polarized progression of differentiation in the vermis anlage. Finally, this developmental defect results in an ataxic gait in some mice.

Key words: FGF, FGF8, FGF17, Fibroblast growth factor, Central nervous system, Cerebellum, Mouse, Neuronal growth factor, Neuronal differentiation factor, Organizer

INTRODUCTION

Patterning of the midbrain-hindbrain (MHB) anlage depends on an ‘organizer’ activity localized at the MHB junction (Alvarez Otero et al., 1993; Hallonet and Le Douarin, 1993; Hallonet and Alvaradomallart, 1997). Classical transplantation experiments demonstrate that MHB tissue can induce midbrain structures when transplanted into the diencephalon and cerebellar tissue when transplanted to the myelencephalon (Gardner and Barald, 1991; Itasaki et al., 1991; Martinez et al., 1991; Bally-Cuif et al., 1992; Marin and Puelles, 1995). Part of the MHB organizer activity has been attributed to FGF8, which is expressed at the MHB junction and can induce ectopic midbrain and cerebellar tissue formation when applied in the diencephalon or midbrain of chick embryos at early somite stages or when ectopically expressed in the midbrain of the mouse (Crossley et al., 1996; Liu et al., 1999; Martinez et al., 1999). This hypothesis has been further supported by an *acerebellar* mutant in zebrafish caused by the loss of *Fgf8* function (Reifers et al., 1998) and by the loss of midbrain and cerebellar tissue in a mouse carrying a severe hypomorphic allele of *Fgf8* (Meyers et al., 1998).

Several families of genes are involved in patterning MHB tissue. *Wnt1*, *Engrailed2* (*En2*) and *Pax5* are essential for specifying midbrain and hindbrain fate before embryonic day 9.5 (E9.5). *Wnt1* null mice, *Pax2/5* double knockout (KO) mice and *Engrailed 1/2* double KO mice all have lost both the mesencephalic vesicle and the cerebellar primordium by embryonic day 10 or earlier (McMahon et al., 1992; Joyner, 1996; Schwarz et al., 1999). Understanding the interaction among these families of genes and their relationship with FGF signaling pathways is essential to delineate the complex genetic program that regulates MHB development. During development, implantation of FGF8 beads into the diencephalon can induce ectopic expression of *Fgf8*, *Wnt1*, *En1*, *En2*, *Pax2* and *Pax5* (Crossley et al., 1996; Sheikh and Mason, 1996; Liu et al., 1999; Shamim et al., 1999). These data suggest that FGF8 may mediate the organizer activity of the MHB junction through the activation and/or maintenance of *Wnt1*, *En2*, *Pax2*, *Pax5* and itself. Recently, FGF8 has been shown to suppress *Otx2* expression at an early somite stage of MHB development (Liu et al., 1999; Martinez et al., 1999), suggesting that FGF8 may also be important for enforcing the midbrain-cerebellar boundary.

In addition to the patterning activity of FGF8, FGF signaling may also regulate the growth and polarity of the midbrain primordium. Overexpression of an *Fgf8* transgene, targeted specifically to the midbrain and MHB junction under the control of a *Wnt1* enhancer (*WEXPZ2-Fgf8*), increased the proliferation of midbrain precursor cells and shifted the high proliferation zone at the caudal part of the midbrain primordium more rostrally (Lee et al., 1997). At the molecular

level, this transgene promoted the expression of *ELF-1* and *En2* at the caudal end of the midbrain and shifted their gradients of expression more rostrally. However, unlike the relatively broad expression domain of the *WEXPZ2-Fgf8* transgene, endogenous *Fgf8* expression is localized primarily in the cerebellar anlage. Thus, although FGF8 may have a significant paracrine effect on the development of adjacent midbrain structures, the role of FGF8 in regulating cerebellar growth and the polarity of cerebellar development remains to be addressed.

FGFs are a large family of at least 19 growth factors sharing 13-71% amino acid identity (pairwise comparisons of mouse or rat FGFs). FGFs are organized into six subfamilies of higher sequence similarity (Coulier et al., 1997; Xu et al., 1999) and members in the same subfamily often share similar biochemical properties. FGFs can activate one of four high-affinity FGF receptor tyrosine kinases, which mediate diverse biological events including ductal branching, cell proliferation, differentiation and migration (Hogan and Yingling, 1998; McKeehan et al., 1998; Naski and Ornitz, 1998; Szebenyi and Fallon, 1999).

Recent expression studies have identified a family of three related *Fgfs* (*Fgf8, Fgf17* and *Fgf18*) in the MHB junction (Maruoka et al., 1998; Xu et al., 1999). This observation raised the question of whether all three FGFs are equivalent in function or whether they have diverged. Divergence could result from altered biochemical properties, such as receptor specificity, from altered temporal and spatial expression patterns or from an altered repertoire of downstream target genes at different stages of development. In this study, we demonstrate that all three *Fgfs* have similar biochemical properties in vitro yet have distinct spatial and temporal patterns of expression in vivo. By disrupting alleles of *Fgf8* and *Fgf17* in mice, we show that these genes have adopted unique yet complementary roles to regulate the size of the medial cerebellar (vermis) anlage and consequently the mature vermis cerebellum. Cellular and genetic evidence supports a functional cooperation between FGF8 and FGF17 and demonstrates that, after E11, these molecules no longer act as an organizer signal but function to regulate cell proliferation and the transition between proliferation and differentiation in the vermis anlage.

MATERIALS AND METHODS

Fgf17 gene targeting vector

A 6.7 kb *Bam*HI-*Eco*RI genomic clone containing exon 1a, 1b, 1c and 2 was used to construct the targeting vector. Exons 1a and 1b were deleted and replaced with a *Sal*I site and a *Sac*II site, between which a cre gene with human β-actin gene polyadenylation sequence (Lewandoski et al., 1997) and a PGK/neo cassette were inserted (Tybulewicz et al., 1991). The targeting construct was then finished by placing this *Bam*HI and *Eco*RI fragment into the pTK1TK2 vector (Chisaka and Capecchi, 1991). SM1 ES cells were transfected with the targeting vector and selected with G418 and FIAU. Antibiotic-resistant clones were screened for homologous recombination using both 5′ and 3′ probes as indicated (Fig. 1).

Generation of *Fgf17*$^{-/-}$, *Fgf8*$^{\Delta 2,3n}$/+ mice

To generate *Fgf17*$^{-/-}$, *Fgf8*$^{\Delta 2,3n}$/+ mice, *Fgf8/17* double heterozygous mice were first obtained by breeding *Fgf17*$^{-/-}$ mice with *Fgf8*$^{\Delta 2,3n}$/+ mice (Meyers et al., 1998). Double heterozygous mice were then mated to *Fgf17*$^{-/-}$ mice to obtain mutants that are heterozygous for the *Fgf8*$^{\Delta 2,3n}$/+ allele in an *Fgf17*$^{-/-}$ background. The *Fgf8*$^{\Delta 2,3n}$/+ allele was identified by Southern blot as previously described (Meyers et al., 1998). All mice were maintained in a 129/sv and C57/B6 mixed genetic background.

Histology and immunohistochemisty

Anti-BrdU immunohistochemistry was carried out as previously described (Naski et al., 1998) with minor modifications. Embryos were labeled by IP injection of pregnant females with BrdU (Sigma Inc.) at a dosage of 100 mg/kg. Embryos were fixed in 4% paraformaldehyde overnight at 4°C and embedded in paraffin. After deparaffinization, rehydration and trypsin digestion, 4 μm sections were incubated with an anti-BrdU monoclonal antibody (Becton-Dickson Inc.) overnight at 4°C, followed by peroxidase immunohistochemistry using the ABC kit and the DAB substrate kit (Vector Lab, Inc). Hematoxylin and eosin staining were carried out by our histology core facility. In all cases, serial sagittal sections covering the medial portion of the cerebellum were collected. Midline sections were identified as those with the thinnest cerebellar neuroepithelium and shortest dorsal-ventral dimension in the cerebellar primordium.

For histological analysis, brains from postnatal day 2 and 2-month-old adult mice were fixed in 4% paraformaldehyde overnight at 4°C and embedded in paraffin. 8 μm sagittal sections were collected and stained with Hematoxylin and eosin.

Calbindin expression was detected with a rabbit polyclonal antibody (Chemicon International, Inc.) and visualized by tyramide signal amplification (NEN life science products).

In situ hybridization

In situ hybridization using ^{35}S-UTP-labeled probes was carried out as previously described (Xu et al., 1999). The plasmids for generating the *Wnt1, En2* and *Pax5* probes were kindly provided by A. P. McMahon, A. L. Joyner and P. Gruss, respectively. Mouse EST AA199520 (Washington University mouse EST project) was used as the template to generate an *Otx2* probe. The template for the *Fgf18* probe, consisting 310 bp of 3′ coding sequence and 360 bp of 3′UTR, was subcloned from a cDNA isolated from a mouse E14.5 embryonic cDNA library (Novagen, Cat. No. 69636-1).

RESULTS

Midbrain and cerebellar tissue loss in mice lacking *Fgf17*

To study the in vivo function of the *Fgf17* gene, an *Fgf17* mutant allele (*Fgf17*^{neo}) was generated through homologous recombination in embryonic stem cells (Fig. 1A,B). In the mutant allele, the translation initiation site and two exons encoding the signal peptide were deleted. Embryonic MHB tissue from mice homozygous for this allele expressed no detectable *Fgf17* mRNA and heterozygous mice had reduced expression of *Fgf17* (Fig. 1C). Therefore, the mutant allele is expected to be a null allele. Homozygous *Fgf17*^{neo}*(Fgf17*$^{-/-}$*)* mice were born alive with the expected Mendelian frequency. They have no gross anatomical abnormalities and appeared healthy. Histological examination of postnatal day 2 (P2) and adult *Fgf17*$^{-/-}$ mice revealed a significant tissue loss in the most caudal part of the midbrain, the inferior colliculus and the vermis cerebellum (Fig. 2). Other regions of the CNS appeared normal (data not shown). In the mouse, the most rostral lobe of the vermis is numbered as lobe III (for consistency with

other organisms such as rat). In *Fgf17*$^{-/-}$ mice, lobe III was roughly one third of normal size. The fissure that separates lobe III and IV failed to form completely, leaving these two lobes partially fused (arrows in Fig. 2B,D). In contrast, the hemispheres of the cerebellum appeared normal in *Fgf17*$^{-/-}$ mice (Fig. 2E,F). In addition, the overall size of the mutant vermis cerebellum is about 82% that of control mice (based on measurement of the area of histological sections). *Fgf17* is thus an essential regulator of vermis cerebellar size.

Temporal separation of *Fgf8*, *Fgf17* and *Fgf18* expression in the MHB junction

Although the MHB tissue loss observed in *Fgf17*$^{-/-}$ mice is readily apparent in all mice (n=5) examined, the phenotype is milder than that observed in a previously reported mouse that is severely hypomorphic for *Fgf8* (*Fgf8*$^{\Delta 2,3}$/*Fgf8*^{neo}) (Meyers et al., 1998). The difference in phenotype may result from spatial and temporal differences in gene expression of *Fgf8*, *Fgf17* and *Fgf18*, from different levels of expression or from different biochemical properties of these FGFs. Previous studies have shown that *Fgf8*, *Fgf17* and *Fgf18* are all expressed in the MHB junction between E9.5 and E10.5 (Maruoka et al., 1998; Xu et al., 1999). However, existing data did not provide a comparative analysis of all three *Fgf*s at stages prior to E9.5 or later than E12.5. To investigate the apparent differences in the function of *Fgf8*, *Fgf17* and potentially *Fgf18*, the spatial and temporal expression patterns of these genes were examined between E8.5 and E14.5. At E8.5 (8-9 somite stage), all three *Fgf*s became detectable in the MHB junction and examination of serial sections showed that *Fgf8* expression clearly covered a broader region than either *Fgf17* or *Fgf18* (Fig. 3Ba-l). By E10.5, all three *Fgf*s were expressed with similar intensity, with *Fgf17* covering the broadest domain along both the mediolateral (data not shown) and rostrocaudal planes (Fig. 3Bm-q). By E12.5, *Fgf8* and *Fgf18* expression intensity became weak, while *Fgf17* expression intensity remained strong (Fig. 3Br-v). By E13.5 (data not shown) and E14.5 (Fig. 3Bw-aa), *Fgf8* and *Fgf18* expression were no longer detectable at the MHB junction while *Fgf17* expression persisted, although with a narrowed expression domain. This analysis and comparison of the phenotypes of *Fgf17*$^{-/-}$ mice and *Fgf8*$^{\Delta 2,3}$/*Fgf8*^{neo} mice suggested that *Fgf17* may have a predominant role at later stages of MHB development and that *Fgf8* is more important at earlier stages of MHB development (Fig. 3C).

FGF8, FGF17 and FGF18 have similar biochemical properties

To compare the biochemical properties of FGF8, FGF17 and FGF18 their receptor specificity and biological activity was examined. Human recombinant FGF1, FGF8, FGF17 and FGF18 were assayed for their ability to stimulate DNA synthesis in receptor-expressing BaF3 cells. Consistent with previously published data (Ornitz et al., 1996), FGF1 induced strong activity in all seven cell lines expressing FGFR1b, FGFR1c, FGFR2b, FGFR2c, FGFR3b, FGFR3c or FGFR4. To assess the relative activity of FGF8, FGF17 and FGF18, FGF1 activity was normalized to 100%, and the activity of FGF8, FGF17 and FGF18 at the same concentration was calculated relative to that of FGF1 (Table 1). This analysis showed that FGF8, FGF17 and FGF18 had strong activity towards FGFR3c and FGFR4c, moderate activity towards FGFR2c, minimal activity towards FGFR1c and no detectable activity towards any b isoform receptor. Together these data indicate that the in vitro receptor specificity and activity for FGF8, FGF17 and FGF18 are very similar; although, accessory molecules still could differentially modify relative activity in vivo. Nevertheless, this analysis suggests that phenotypic differences between *Fgf8*$^{\Delta 2,3n}$/*Fgf8*^{neo} mice and *Fgf17*$^{-/-}$ mice are due to differences in their spatial and temporal expression patterns in the MHB junction.

Alleles of *Fgf17* and *Fgf8* are not identical but can cooperate to regulate cerebellar size

Because *Fgf8* and *Fgf17* overlap in their pattern of expression between E8.5 and E12.5, it was important to address the question of whether alleles of *Fgf8* and *Fgf17* have equivalent or redundant function. Mice containing null alleles of both genes (*Fgf17*$^{-/+}$, *Fgf8*$^{\Delta 2,3n}$/+) were generated by mating *Fgf17*$^{-/-}$ mice with mice carrying an *Fgf8* null allele, *Fgf8*$^{\Delta 2,3n}$/+, (Meyers et al., 1998). If an allele of *Fgf8* could

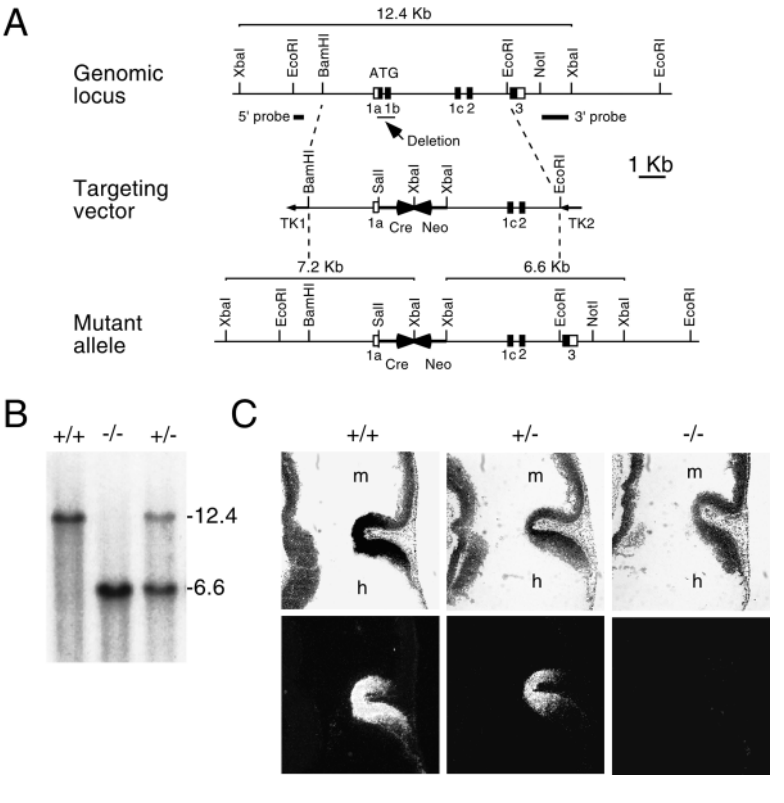

Fig. 1. Generation of a *Fgf17*-null allele. (A) A schematic representation of the *Fgf17* genomic locus, the targeting vector and the mutant allele generated following homologous recombination. (B) Southern blot identification of the *Fgf17* mutant allele. The 3′ probe (as indicated in A) identifies the wild-type allele as a 12.4 kb *Xba*I fragment and the mutant allele as a 6.6 kb *Xba*I band. (C) In situ hybridization analysis of *Fgf17* expression in the midbrain-hindbrain junction at E11.5. Note that the heterozygous tissue has reduced expression of *Fgf17* compared to that of wild-type tissue while the homozygous mutant has no detectable *Fgf17* transcript. m, midbrain; h, hindbrain.

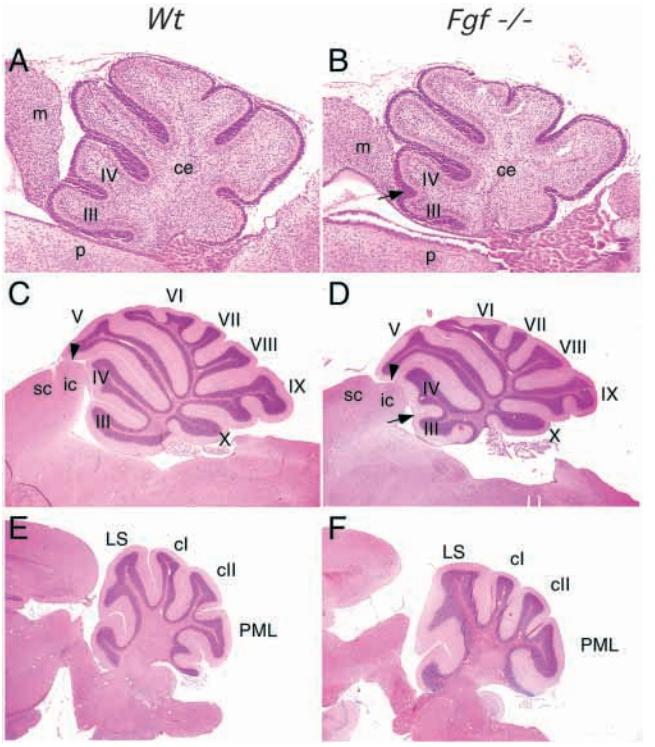

Fig. 2. Histological analysis of the midbrain and cerebellum in wild-type and *Fgf17*$^{-/-}$ mice. Midsagittal (A-D) and parasagittal (E,F) sections of mouse brains stained with Hematoxylin and eosin. (A,B) Postnatal day 2 (P2) mice; (C-F) 2-month-old mice. The genotypes are indicated on the top. Note that in both P2 and adult cerebellum, vermis lobe III in the *Fgf17*$^{-/-}$ tissue (B,D) is one third the size of wild-type tissue (A,C). Arrows in B and D indicate the incomplete formation of the fissure between lobe III and IV. The overall sizes of the vermis and the inferior colliculus (arrow head) are also smaller in tissue from *Fgf17*$^{-/-}$ mice. No tissue loss is observed in the cerebellar hemisphere of *Fgf17*$^{-/-}$ mice (F) compared to wild-type tissue (E). m, midbrain. ce, cerebellum. p, pons. III, IV, V, VI, VII, VIII, IX, X, vermian lobes. sc, superior colliculus. ic, inferior colliculus. LS, lobulus simplex. cI, crus I. cII, crus II. PML, paramedian lobule. Magnification is 50× in A and B and 12.5× in C-F.

substitute for an allele of *Fgf17* then the prediction would be that double heterozygous mice would have a similar phenotype to *Fgf17*$^{-/-}$ mice. Histological analysis did not identify any tissue loss in the MHB of P2 or adult double heterozygous mice (compare Fig. 4A and C to Fig. 2A and C). This demonstrates that one allele of *Fgf17* is not equivalent to one allele of *Fgf8*, and that *Fgf17* has a unique role during MHB development.

By crossing double heterozygous mice with *Fgf17*$^{-/-}$ mice, a compound mutant that is heterozygous-null for *Fgf8* in an *Fgf17*-null background (*Fgf17*$^{-/-}$, *Fgf8*$^{\Delta 2,3n}$/+) was generated. Histological analysis showed that at both neonatal (P2) and adult stages, vermis lobe III is completely lost in all *Fgf17*$^{-/-}$, *Fgf8*$^{\Delta 2,3n}$/+ mice analyzed (*n*=4) (Fig. 4B,D) and that there is a further progressive decrease in the overall size of the vermis cerebellum compared to that of wild-type mice (~76%). Tissue loss in the inferior colliculus is similar to that in *Fgf17*$^{-/-}$ mice (compare Figs 2D and 4D). Therefore, the loss of an additional allele of *Fgf8* can significantly increase the cerebellar tissue loss observed in *Fgf17*$^{-/-}$ mice demonstrating that these genes

Table 1. Relative mitogenic activity* of FGF1, FGF8, FGF17 and FGF18

	FGF ligand*			
FGFR	FGF1‡ ±s.d.	FGF8 ±s.d.	FGF17 ±s.d	FGF18 ±s.d.
1c	100±5.6	1.4±0.5	2.7±0.4	2.2±0.4
2c	100±4.1	20.6±3.6	53.8±3.8	7.4±0.4
3c	100±25.3	43.9±1.4	89.2±1.1	22.3±3.2
4Δ	100±17.9	64.6±1.2	95.1±5.7	78.3±1.6
1b	100±4.2	4.4±0.6	5.7±0.1	6.1±1.8
2b	100±5.4	5.9±0.6	5.1±0.9	5.3±0.6
3b	100±1.4	2.2±0.4	2.0±0.5	2.5±0.3

*These data represent relative activity to FGF1 at a concentration of 156 pM

‡FGF1 activity is normalized to 100 percent for each cell line.

do have some redundant function. Interestingly, like in *Fgf17*$^{-/-}$ mice, the cerebellar phenotype in *Fgf17*$^{-/-}$, *Fgf8*$^{\Delta 2,3n}$/+ mice is limited to the midline vermis and the hemispheres of the cerebellum are unaffected (Fig. 4E,F).

FGF17 and FGF8 do not specify cell identity in the MHB junction at E12.5

Early in MHB development *Fgf8* can induce and maintain expression patterns of genes that specify the identity of the MHB region, a property often referred to as organizer activity. Specifically, FGF8 can induce and maintain the expression of *Wnt1*, *En1*, *En2*, *Pax2* and *Pax5* at the 8- to 12-somite stage of development (E8.5-9.5 in mice) (Crossley et al., 1996; Liu et al., 1999; Shamim et al., 1999). To test whether partial loss of FGF signals between E8.5 and E12.5 affect patterning of the vermis anlage, the expression of *Wnt1*, *En2*, *Pax5* and *Otx2* were compared at E12.5 in wild-type and *Fgf17*$^{-/-}$, *Fgf8*$^{\Delta 2,3n}$/+ mice. In tissue from *Fgf17*$^{-/-}$, *Fgf8*$^{\Delta 2,3n}$/+ mice, there was no significant change in either the spatial pattern or the level of expression of *Wnt1*, *En2* or *Pax5*. *Otx2*, which is negatively regulated by FGF8 at early somite stages, also did not change in MHB tissue from *Fgf17*$^{-/-}$, *Fgf8*$^{\Delta 2,3n}$/+ mice at this stage (Fig. 5). RNA blot analysis of dissected midbrain and anterior hindbrain tissue showed no quantitative changes in the expression of these genes (data not shown). These data demonstrate that loss of FGF8 and FGF17 activity prior to E12.5 does not cumulatively affect the patterning of the MHB region at E12.5.

Decreased proliferation of cerebellar precursor cells in mice lacking alleles of *Fgf8* and *Fgf17*

The extent of MHB tissue loss observed at postnatal day 2 (P2) was similar to that of adult *Fgf17*$^{-/-}$ mice and *Fgf17*$^{-/-}$, *Fgf8*$^{\Delta 2,3n}$/+ mice suggesting an early developmental origin of the phenotype. To examine whether a defect in cell proliferation or cell death could account for the observed tissue loss, BrdU-labeling indices were examined at embryonic ages E10.5 to E12.5 and TUNEL assays were examined at E12.5 (Fig. 6 and data not shown). Anti-BrdU immunohistochemistry was focused on midline sagittal sections (see methods for details) because it has been documented that the primordium for the anterior vermis is located at the most medial part of the cerebellar plate (Altman and Bayer, 1997). The number of BrdU-positive and BrdU-negative cells in the entire midline

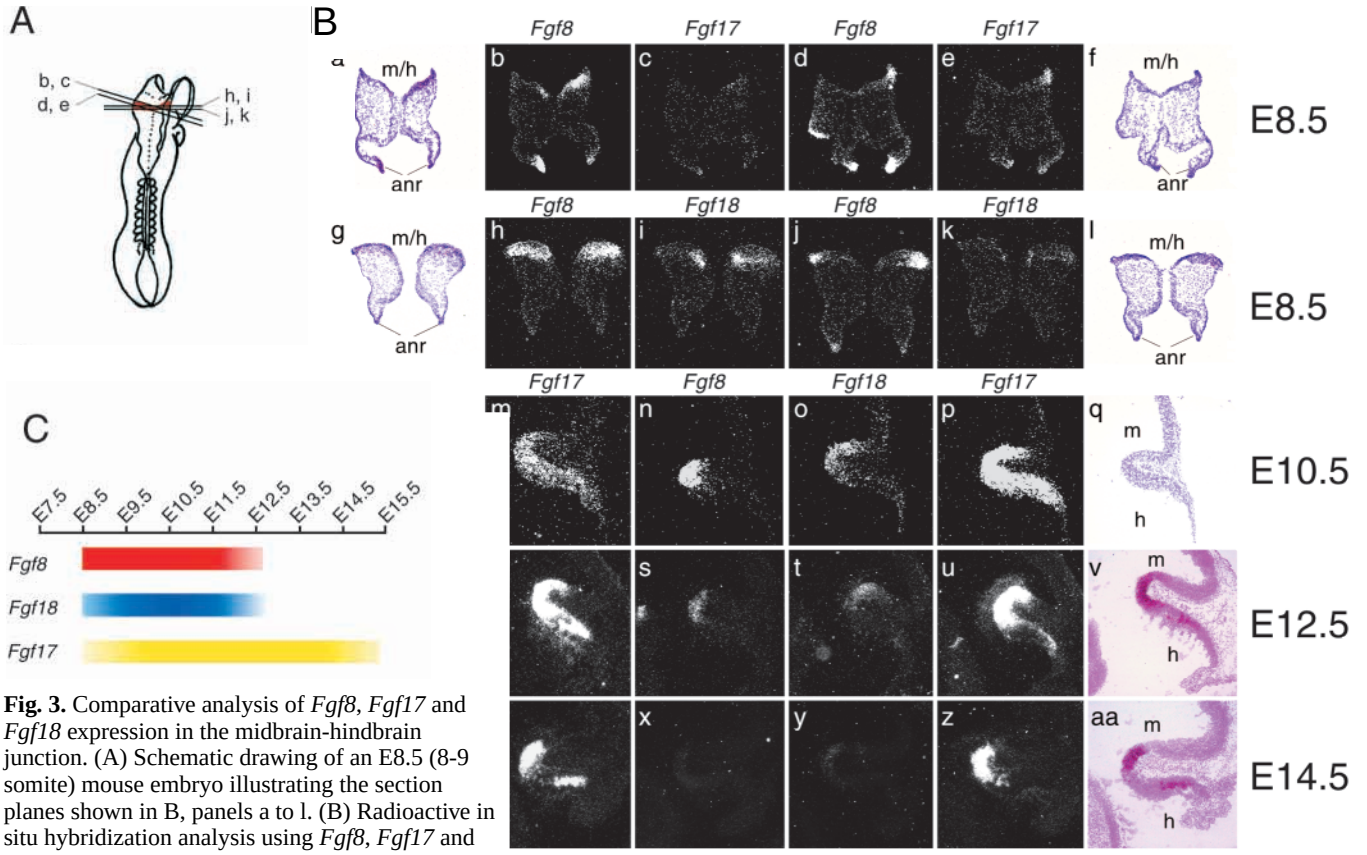

Fig. 3. Comparative analysis of *Fgf8*, *Fgf17* and *Fgf18* expression in the midbrain-hindbrain junction. (A) Schematic drawing of an E8.5 (8-9 somite) mouse embryo illustrating the section planes shown in B, panels a to l. (B) Radioactive in situ hybridization analysis using *Fgf8*, *Fgf17* and *Fgf18* RNA probes on transverse (a-l) or sagittal (m-aa) serial sections. Embryo ages are indicated on the right. The probes used are indicated. a, f, g, i, q, v and aa show corresponding bright-field images of panels b, e, h, k, o, r and w. (b,c) Two adjacent sections through the edge of the isthmus showing strong *Fgf8* expression but no *Fgf17* expression. (d,e) Two adjacent sections through the center of the isthmus showing strong *Fgf8* expression but weaker *Fgf17* expression. (h,i) Two adjacent sections through the center of the isthmus showing strong *Fgf8* expression but weaker *Fgf18* expression. (j,k) Two adjacent sections through the edge of the isthmus showing strong *Fgf8* expression but no *Fgf18* expression. (m-p) Serial midline sections showing similar expression intensity of *Fgf8*, *Fgf17* and *Fgf18*. Note that *Fgf17* has the broadest expression domain by E10.5. (r-u) Serial midline sections showing strong expression of *Fgf17* but weak expression of *Fgf8* and *Fgf18* at E12.5. (w-z) Serial midline sections showing strong *Fgf17* expression but no *Fgf8* and *Fgf18* expression at E14.5. (C) A schematic summary of the temporal difference in *Fgf8*, *Fgf17* and *Fgf18* expression described in B and in data not shown. Weak signals are presented with fading color. Note that the expression of *Fgf17* extends beyond that of *Fgf8* and *18* beginning at E12.5 and extending through E14.5 and that *Fgf8* expression predominates at E8.5.

primordium were quantified at E10.5, E11.5 and E12.5. At E10.5, no significant difference in cell proliferation indices or cellular morphology of the cerebellar neuroepithelium was detected (Fig. 6Aa-c) and in all genotypes the proliferation index was about 42% (Fig. 6B). By E11.5, the proliferation index of both wild-type and *Fgf17*$^{-/-}$ tissue was 40.8±0.2 % (Fig. 6Ad-e,B); however, the proliferation rate in tissue from *Fgf17*$^{-/-}$, *Fgf8*$^{\Delta 2,3n}$/+ embryos decreased to 31.7±0.3% (Fig. 6Af,B), significantly lower than in tissue from either wild-type or *Fgf17*$^{-/-}$ mice. Consistent with the proliferation data, the cerebellar neuroepithelium in *Fgf17*$^{-/-}$, *Fgf8*$^{\Delta 2,3n}$/+ mice was thinner than in either *Fgf17*$^{-/-}$ mice or wild-type mice (Fig. 6Ad-f). By E12.5, the proliferation rate in the wild-type vermis decreased to 30.1±1.5%, in *Fgf17*$^{-/-}$ tissue it decreased further to 18.8±1.7%, and in tissue from *Fgf17*$^{-/-}$, *Fgf8*$^{\Delta 2,3n}$/+ embryos the proliferation index was only 14.1±2.2% (Fig. 6Ag-I,B). These data indicate a progressive decrease in cell proliferation in the *Fgf*17$^{-/-}$ and *Fgf17*$^{-/-}$, *Fgf8*$^{\Delta 2,3n}$/+ mice compared to wild-type mice. A consequence of the decreased proliferation index is that by E12.5 the midline cerebellar neuroepithelium in *Fgf17*$^{-/-}$, *Fgf8*$^{\Delta 2,3n}$/+ mice and to a lesser extent in *Fgf17*$^{-/-}$ mice was thinner than that of wild-type mice (Fig. 6Ag-i). Significantly, the decrease in proliferation was only observed at stages when the expressions of all three *Fgfs* were declining, suggesting a more significant redundancy at stages prior to E11.5. At E12.5, TUNEL analysis showed that cell death occurred in less than 1% of neuroepithelial cells in the vermis anlage in both wild-type and *Fgf17*$^{-/-}$, *Fgf8*$^{\Delta 2,3n}$/+ mice (data not shown). In summary, these data demonstrate that, after E11, FGF8, FGF17 and possibly FGF18 act as growth factors that maintain proliferation but not cell survival of precursor cells in the midline of the cerebellar primordium.

Advanced migration and differentiation of postmitotic Purkinje cells in embryos lacking *Fgf8* and *Fgf17*

Purkinje cells in the mouse cerebellar primordium stop proliferation and begin to differentiate at E13 to E14 (for review see Hatten and Heintz, 1995), coincident with the termination of *Fgf8* and *Fgf18* expression and with the

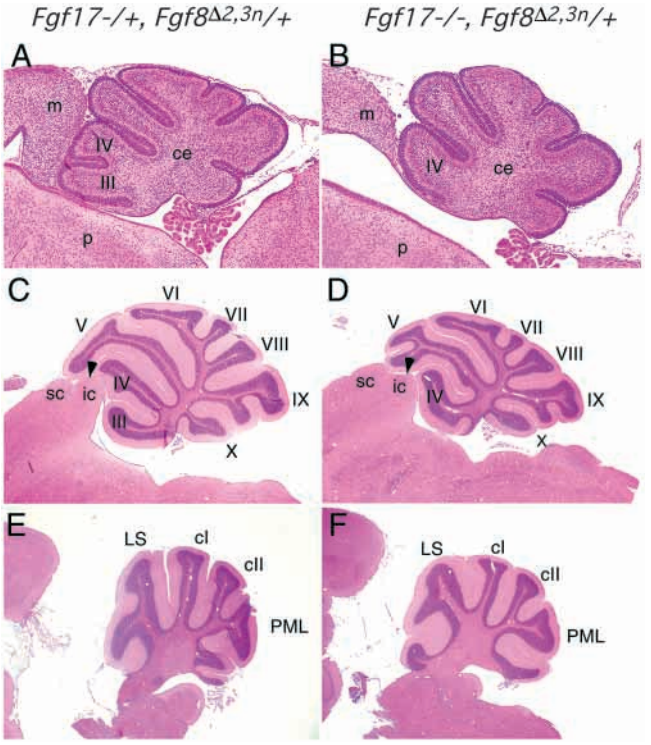

Fig. 4. Histological analysis of the midbrain and cerebellum from *Fgf17*$^{-/+}$, *Fgf8*$^{\Delta 2,3n}$/+ and *Fgf17*$^{-/-}$, *Fgf8*$^{\Delta 2,3n}$/+ mice. (A-D) Midsagittal and (E,F) parasagittal sections of mouse brains stained with Hematoxylin and eosin. (A,B) Postnatal day 2 (P2) mice; (C-F) 2-month-old mice. The genotypes are indicated on the top. Note that, in both P2 and adult cerebellum, vermis lobe III in the *Fgf17*$^{-/-}$, *Fgf8*$^{\Delta 2,3n}$/+ mice is completely missing, and the overall sizes of the inferior colliculus and the cerebellum are also smaller than double heterozygous tissue or *Fgf17*$^{-/-}$ tissue (see Fig. 2). In contrast, the midbrain and cerebellum in *Fgf17*$^{-/+}$, *Fgf8*$^{\Delta 2,3n}$/+ mice is normal compared to that in wild type (see Fig. 2A,C). No tissue loss is observed in the hemispheres in both *Fgf17*$^{-/+}$, *Fgf8*$^{\Delta 2,3n}$/+ mice (E) and *Fgf17*$^{-/-}$, *Fgf8*$^{\Delta 2,3n}$/+ mice (F). Abbreviations are as in Fig. 2. Magnification is ×50 in A and B and ×12.5 in C-F.

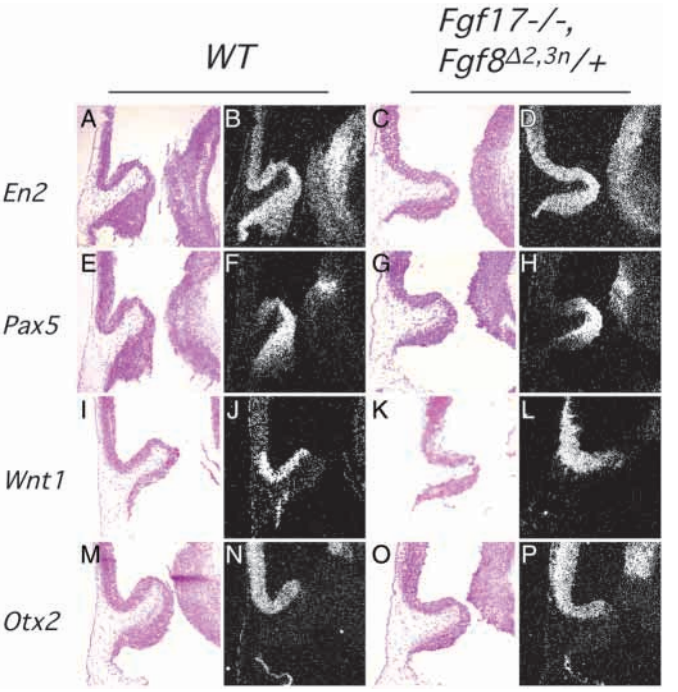

Fig. 5. Expression of midbrain-hindbrain specific genes at E12.5. Frozen sections from wild-type (left) and *Fgf17*$^{-/-}$, *Fgf8*$^{\Delta 2,3n}$/+ embryos (right) were hybridized with ^{35}S-UTP-labeled *En2* (A,D), *Pax5* (E,H), *Wnt1* (I,L) and *Otx2* (M,P) probes (as indicated). For each dark-field image, the corresponding bright-field image is shown on its left. Note that there is no difference in the expression pattern or intensity of these genes between wild-type and mutant embryos.

significant reduction in *Fgf17* expression (Fig. 3). These observations suggest a possible role for FGFs in regulating the transition from proliferation to differentiation in the vermis. The onset of Purkinje cell differentiation is highlighted by extensive radial migration from the neuroepithelium and the expression of calbindin, a specific marker of the Purkinje cell lineage in the cerebellar anlage (Altman and Bayer, 1985, 1997; Yuasa et al., 1991). Additionally, thymidine radiographic studies have established that Purkinje cell migration is polarized and proceeds in a caudal-lateral to rostral-medial direction (Altman and Bayer, 1985, 1997), and that migrating Purkinje cells form a morphologically distinct layer of cells adjacent to the neuroepithelium in a domain called the cortical transitory zone (ctz) (Altman and Bayer, 1985) (Fig. 7A-D). Histological analysis of wild-type embryos showed that, at E14, midline sagittal sections showed no evidence of Purkinje cell migration (Fig. 7B). However, on sections 60-80 μm from the midline the ctz began to form (Fig. 7C) and in lateral sagittal sections, Purkinje cells have migrated progressively deeper into the cortical zone (cz) (Fig. 7D). These data indicate that at E14 Purkinje cell differentiation has not extended to the most medial portion of the vermis primordium.

To investigate the relationship between proliferation and differentiation, the timing of the formation of the ctz in wild-type embryos was examined by comparing 1 hour and 48 hours BrdU labeling. In embryos labeled for 1 hour at E14, cells in the neuroepithelium are BrdU-positive whereas all migrating cells in the ctz are BrdU-negative (Fig. 7E). However, if the embryos are labeled at E12.5 and harvested 2 days later, the cells in the ctz, but not those in the cortical zone (cz) at the caudal part of the vermis primordium are labeled with BrdU (Fig. 7F). These data demonstrate that the migratory cells in the ctz exited the cell cycle after E12.5, while migratory cells that have moved into the cz at the caudal and lateral part of the primordium exited the cell cycle prior to E12.5. Therefore, the ctz marks the most recent differentiation field, and the relative position of the ctz along the medial-lateral axis indicates the extent of differentiation.

Histological analysis of serial sagittal sections from E14 *Fgf17*$^{-/-}$ and *Fgf17*$^{-/-}$, *Fgf8*$^{\Delta 2,3n}$/+ embryos showed that a ctz had clearly formed in the midline at the caudal part of the cerebellar primordium indicating that Purkinje cell migration has already begun in the most medial portion of the vermis anlage by E14 (Fig. 7G,H). Variations seen within stage-matched embryos are presented in Table 2.

Collectively, these data show that Purkinje cell differentiation has progressed rostrally in *Fgf17*$^{-/-}$ mice and that differentiation was even more advanced in *Fgf17*$^{-/-}$,

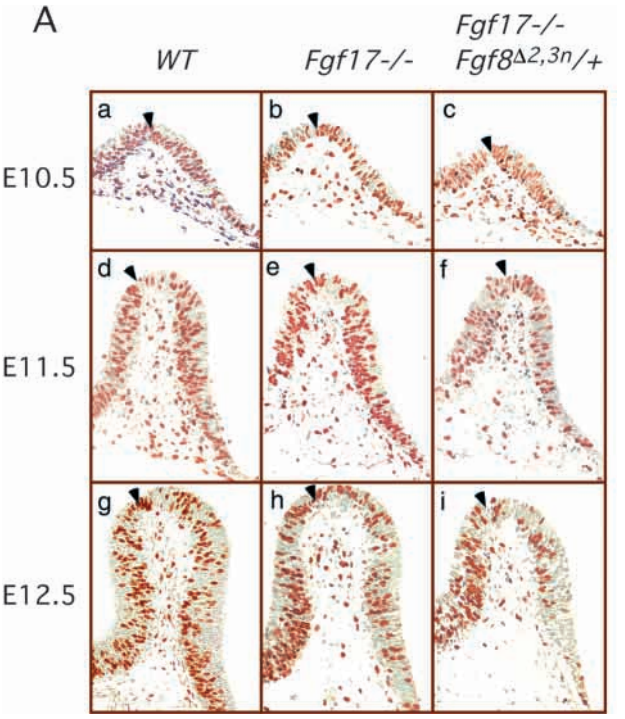

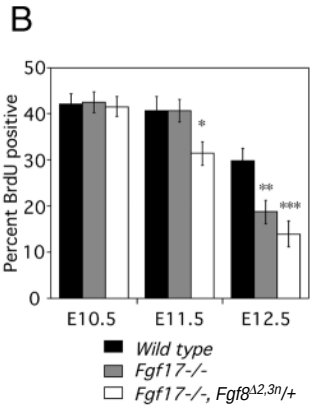

Fig. 6. Neuroepithelial proliferation in the midline cerebellar anlage. (A) Representative midsagittal sections of the midbrain and cerebellar primordium derived from E10.5 (a-c), E11.5 (d-f) and E12.5 (g-i) embryos that have been labeled with BrdU for 1 hour in utero. The sections were incubated with an anti-BrdU antibody and BrdU-positive cells were visualized with horseradish peroxidase immunohistochemistry using DAB as the substrate. Slides were counterstained with 0.1% Methyl Green. In all sections, the midbrain vesicle is to the left and the hindbrain vesicle is to the right. Arrowheads indicate the physical boundaries between the midbrain and cerebellar primordia. (B) Quantification of the percentage of BrdU-positive cells in wild-type, *Fgf17*$^{-/-}$ and *Fgf17*$^{-/-}$, *Fgf8*$^{\Delta 2,3n}$/+ embryos at E10.5, E11.5 and E12.5. The symbols for the different genotypes are indicated. Each bar presents data from 3 embryos, and 4-6 sections were analyzed for each embryo. Error bar represent standard deviation. *, significantly lower than wild-type (P=0.002) and *Fgf17*$^{-/-}$ mice (P< 0.0001). **, significantly lower than wild type (P= 0.001). ***, significantly lower than wild-type (P=0.0005) and *Fgf17*$^{-/-}$ mice (P=0.043). Statistical analysis is done using ANOVA with Statview 4.5 software. Magnification in A is ×100.

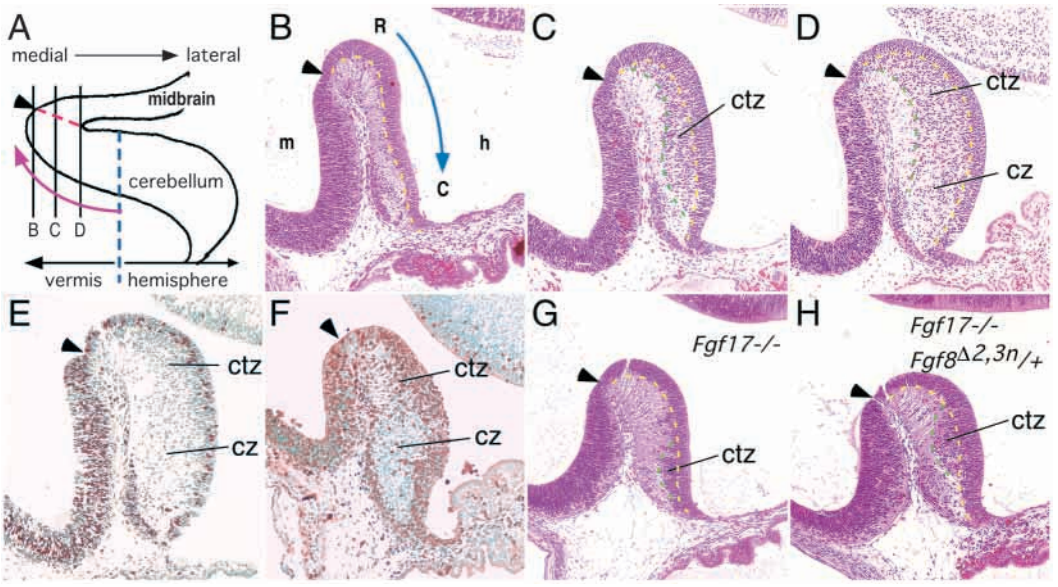

Fig. 7. Purkinje cell migration in the cerebellar vermis primordium at E14. (A) A schematic coronal view of a wild-type hemicerebellar primordium showing the section planes for B-D, which progress from medial to lateral. Dashed red line and arrowhead indicate the boundary between the midbrain and the cerebellum in all panels. Dashed blue line marks the presumptive boundary between vermis and hemisphere cerebellar primordia. Purple arrows indicates the progression of Purkinje cell differentiation from caudal-lateral to rostral-medial. (B-D) H&E-stained sagittal sections through wild-type cerebellar vermis anlage. (B) Midline section showing no cell migration from the neuroepithelium. Blue arrow shows the rostral-to-caudal axis. (C) Section 60 μm from the midline showing migratory cells in the cortical transitory zone (ctz). (D) Section 120μm from the midline showing migratory cells in the ctz and the cortical zone (cz). (E,F) Anti-BrdU immunohistochemistry of BrdU-labeled parasagittal sections (~60-100 μm from the midline) through the MHB junction from wild-type E14 embryos. Both sections are slightly tilted to give more representation to the cortical zone in the lateral portion of the cerebellum. (E) BrdU-labeled in utero 1 hour before harvest. (F) BrdU-labeled at E12 and harvested at E14. (G,H) H&E-stained mid-sagittal sections showing the formation of a ctz at the caudal part of the vermis primordium in *Fgf17*$^{-/-}$ tissue (G) and the formation of a ctz extending into the anterior half of the vermis primordium in *Fgf17*$^{-/-}$, *Fgf8*$^{\Delta 2,3n}$/+ tissue (H). The yellow dashed line shows the dorsal edge of the neuroepithelium and the green dashed line shows the front of cell migration. R, rostral. C, caudal. m, midbrain vesicle. h, hindbrain vesicle. Magnification in B-H is ×50.

Fgf8$^{\Delta 2,3n}$/+ mice. In *Fgf17*$^{-/-}$, *Fgf8*$^{\Delta 2,3n}$/+ mice, the ctz not only formed at the midline in all embryos examined (6 of 6), but also in most cases (5 of 6), had extended into the rostral half of the vermis anlage (Fig. 7H, Table 2).

Calbindin is the earliest known marker for the Purkinje cell lineage and its expression increases as differentiation progresses (Yuasa et al., 1991). To further evaluate the progression of Purkinje cell differentiation, Calbindin

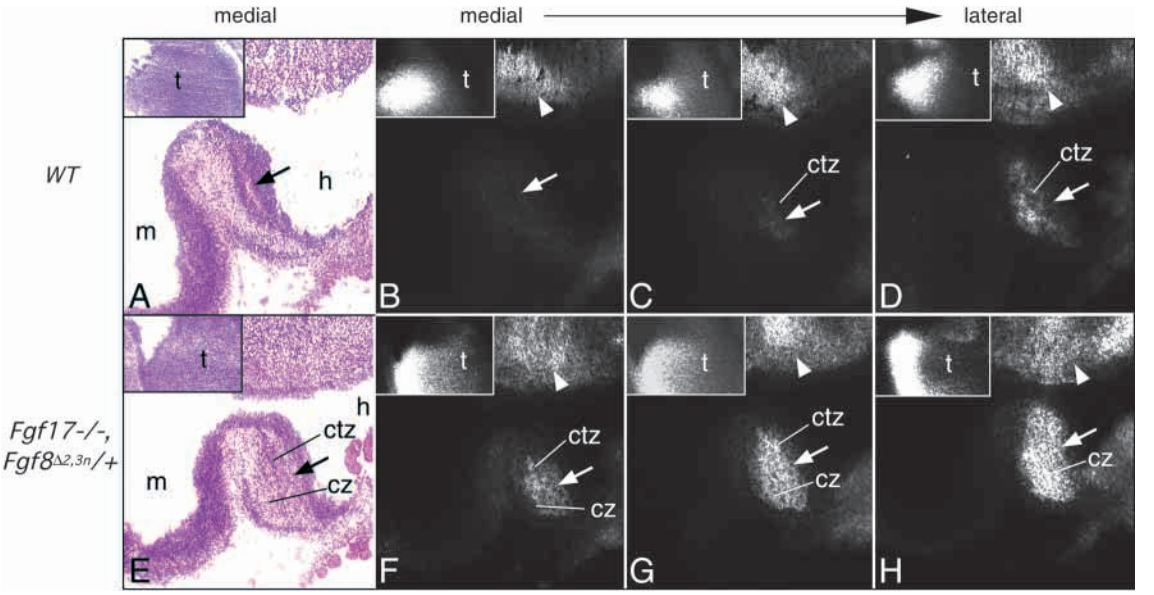

Fig. 8. Calbindin expression in the cerebellar vermis primordium at E14.5. Immunofluorescent staining for calbindin expression in wild-type (B-D) and *Fgf17*$^{-/-}$, *Fgf8*$^{\Delta 2,3n}$/+ (F-H) MHB tissue. (A,E) H&E-stained images of D and H; (B,F) midline section. (C,G) Sections 30-40 μm from the midline; (D,H) sections 70-80 μm from the midline. Arrows indicate calbindin-positive cells seen in tissue from *Fgf17*$^{-/-}$, *Fgf8*$^{\Delta 2,3n}$/+ embryos and corresponding regions of wild-type embryos. Note that calbindin expression is not detected in the midline of wild-type tissue but is strongly expressed in *Fgf17*$^{-/-}$, *Fgf8*$^{\Delta 2,3n}$/+ tissue. Arrowheads and inserts indicate that wild-type and mutant embryos have similar calbindin staining in the ventral hindbrain (arrowhead) and thalamus (inserts). ctz, cortical transitory zone. cz, cortical zone. t, thalamus. m, midbrain vesicle. h, hindbrain vesicle. Magnification in A-H is ×50.

Table 2. Analysis of cell migration in the midline cerebellar primordium

	WT (*n*=7)	*Fgf17*$^{-/-}$ (*n*=7)	*Fgf17*$^{-/-}$, *Fgf8*$^{\Delta 2,3n}$/+ (*n*=6)
Cell migration observed in the ctz*	0	6	6
Migration restricted to the caudal region	0	5	1
Migration extending into the rostral region	0	1	5

*Cortical transitory zone

expression was examined in the MHB junction at E14.5. In wild-type embryos, the most medial portion of the cerebellar primordium was calbindin-negative (Fig. 8A-C). Calbindin-positive cells were first detectable in sections ~80 μm away from the midline (Fig. 8D). In contrast, in the most medial portion of the cerebellar primordium of *Fgf17*$^{-/-}$, *Fgf8*$^{\Delta 2,3n}$/+ mice, there was strong calbindin expression in the ctz and the cz (Fig. 8E-G). In the lateral part of the vermis primordium, there was a much larger and more intense calbindin-positive domain compared to wild type (compare Fig. 8H with 8D). These data, and the histological analysis, suggest that premature differentiation occurred in the medial portion of the vermis primordium as a consequence of decreased FGF signaling.

Gait defect in *Fgf17*$^{-/-}$, *Fgf8*$^{\Delta 2,3n}$/+ mice

The vermis cerebellum has been functionally associated with motor coordination and maintenance of body equilibrium (Victor et al., 1959; Brodal, 1998). Gait patterns of 3- to 4-month-old wild-type (*n*=8) and *Fgf17*$^{-/-}$ mice (*n*=8) showed a normal symmetric gait, characterized by the overlapping of

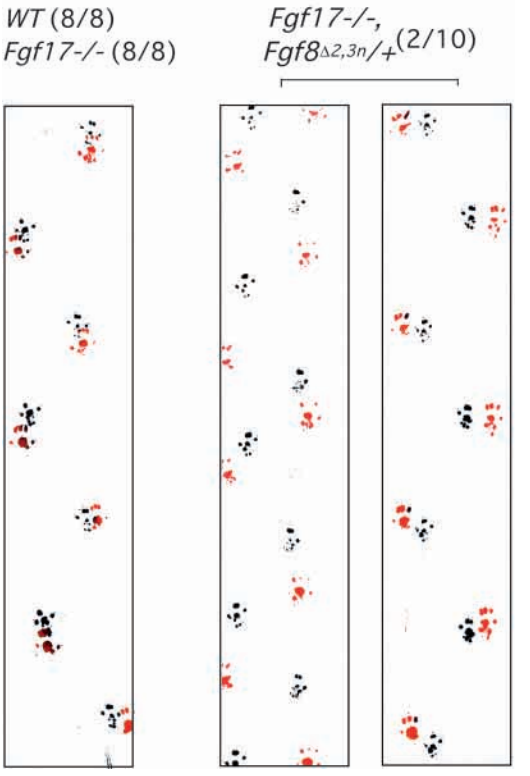

Fig. 9. Gait analysis of wild-type, *Fgf17*$^{-/-}$ and *Fgf17*$^{-/-}$, *Fgf8*$^{\Delta 2,3n}$/+ mice. Paw prints of mice walking through a tunnel (5 cm × 5 cm) on filter paper. Front paws are dipped in black ink and rear paws are dipped in red ink. Note that in wild-type and *Fgf17*$^{-/-}$ mice the front and rear paw prints overlap and that in 2 of 10 *Fgf17*$^{-/-}$, *Fgf8*$^{\Delta 2,3n}$/+ mice the rear paw prints either lag or are lateral to the front paw prints.

hindlimb and forelimbs paw prints (Fig. 9 left). However, two of ten *Fgf17*$^{-/-}$, *Fgf8*$^{\Delta 2,3n}$/+ mice exhibited asymmetric gait patterns characterized by lagging of the hindlimbs (Fig. 9 center) or a wider spread between the hindlimbs (Fig. 9 right). The low penetrance of this phenotype indicates that either the functional consequence of tissue loss in the vermis is subtle or that functional compensation by other regions of the CNS occurs by 3-4 months of age. Because such compensation may be less effective in younger mice, further studies will be required to examine cerebellar function throughout postnatal development.

DISCUSSION

Dose-dependent regulation of vermis growth by FGF

FGF8 is thought to be the signal that mediates MHB organizer function at early somite (6-12 somite) stages, consistent with its expression at that time of development. However, recent expression data (Maruoka et al., 1998; Xu et al., 1999; Fig. 3) showed that two other related *Fgf*s, *Fgf17* and *Fgf18*, are also expressed in the MHB junction and that the expression of all three *Fgf*s, especially that of *Fgf17*, extended into the growth and differentiation phases of cerebellar development. Therefore, it became important to address the function of this family of FGFs at later stages of cerebellar development. BrdU-labeling studies indicated that the peak of cerebellar growth occurred at E10.5-E11.5, because more than 40% of the neuroepithelial cells in the cerebellar primordium were in S-phase at this time, and there is a rapid increase in the total number of cells (more than 5 fold, data not shown) in this region from E10.5 to E12.5. The peak in neuroepithelial cell proliferation 2 days after the onset of *Fgf8* expression suggests that the MHB tissue loss observed in mice carrying hypomorphic alleles of *Fgf8* is caused primarily by a patterning defect prior to E9.5 (Meyers et al., 1998). In contrast, the MHB tissue loss in the *Fgf17*$^{-/-}$ mice and in *Fgf17*$^{-/-}$, *Fgf8*$^{\Delta 2,3n}$/+ mice reported here are likely the direct result of decreased proliferation and/or a subtle patterning defect affecting only the rostral vermis. A major primary defect in morphogenesis was ruled out by the observation that genes essential for patterning the MHB region were expressed in normal patterns in both types of mutants. In addition, histology of the cerebellar primordium of *Fgf*-deficient mice did not exhibit any abnormalities until E12.5 when the midline neuroepithelium in *Fgf17*$^{-/-}$, *Fgf8*$^{\Delta 2,3n}$/+ mice became thinner than that of wild-type neuroepithelium. Moreover, a growth defect is suggested by the significant reduction of BrdU-labeling indices in *Fgf17*$^{-/-}$ and *Fgf17*$^{-/-}$, *Fgf8*$^{\Delta 2,3n}$/+ mice at E11.5 and E12.5. These data also demonstrate that FGF8 and FGF17 act together at these stages because compared to the *Fgf17*$^{-/-}$ mouse, the *Fgf17*$^{-/-}$, *Fgf8*$^{\Delta 2,3n}$/+ mutant is more severely affected both in terms of a decreased cell proliferation index and in terms of the final size of the mature cerebellum. After E11, growth of the vermis anlage is therefore regulated by FGF signals in a dose-dependent manner, which are distinct from their role as an organizer signal 2-3 days earlier in development. It is important to note that the posterior half of the vermis is also reduced in size, although much less than the anterior half. This is most likely due to decreased proliferation at earlier stages of development (before E11.5) in precursor pools of cells that will

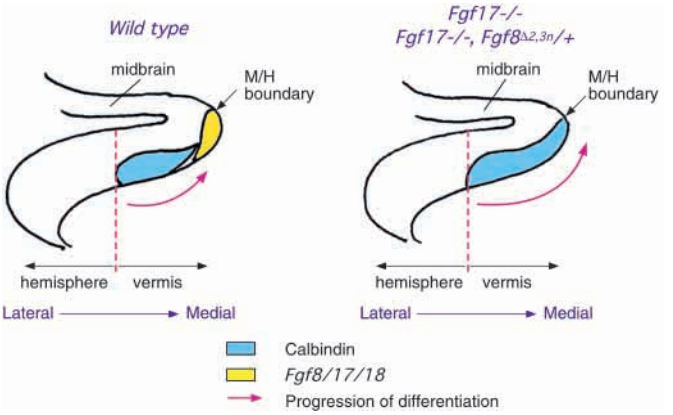

Fig. 10. Model showing the role of FGF signaling for regulating the progression of differentiation in the vermis primordium at E12-14. The diagrams represent coronal views of hemicerebellar primordia. In wild-type tissue (left), localized expression of *Fgf8*, *Fgf17* and *Fgf18* (yellow) inhibits Purkinje cell differentiation, which progresses from caudal-lateral to rostral-medial (pink arrow). Purkinje cell differentiation is highlighted by calbindin expression shown in blue. In the *Fgf17*$^{-/-}$ and *Fgf17*$^{-/-}$, *Fgf8*$^{\Delta 2,3n}$/+ embryos, the premature decrease and the subsequent termination of FGF signaling in the medial vermis anlage results in accelerated rostral-medial progression of Purkinje cell differentiation.

populate both the anterior and posterior vermis. The more severely affected anterior vermis is likely to result from a more significant proliferation defect at later stages of development (E11.5-14). Because the vermis develops in a caudal to rostral orientation (Altman and Bayer, 1985, 1997) decreased neuroepithelial proliferation late in development should predominantly affect the population of cells that give rise to the rostral vermis.

Although the loss of the rostralmost lobes of the vermis appears to mimic a patterning defect, our model proposes that it is more likely attributable to premature exhaustion of the precursor pool of cells giving rise to this tissue. Nevertheless, it remains possible that part of the midline vermis fails to develop in *Fgf17*$^{-/-}$, *Fgf8*$^{\Delta 2,3n}$/+ mice and that the tissue that we observe in the midline is derived from more lateral tissue that now occupies a midline position.

Temporal separation of *Fgf8* and *Fgf17* function in midbrain and cerebellar development

As discussed, the *Fgf17*$^{-/-}$ mice and the *Fgf17*$^{-/-}$, *Fgf8*$^{\Delta 2,3n}$/+ mice have a defect specific to the late phase of cerebellar development. We believe that this is caused by a temporal separation of FGF8 and FGF17 function. The expression patterns shown here suggest that FGF8 dominates at early somite stages, while FGF17 dominates after E11.5. Because FGF8, FGF17 and FGF18 have similar biochemical properties, the difference in temporal expression patterns is more likely to account for the phenotypic difference between mice carrying hypomorphic alleles of *Fgf8* and mice lacking *Fgf17*. The expression patterns also predict a strong redundancy among these FGFs at E9.5-E11.5, which was partially revealed by the more severe phenotype of *Fgf17*$^{-/-}$, *Fgf8*$^{\Delta 2,3n}$/+ mice. In the future, the redundancy may be further examined by generating and analyzing mice lacking additional alleles of *Fgf18*.

Because *Fgf18* expression is not detected during gastrulation, *Fgf17*$^{-/-}$, *Fgf8*$^{\Delta 2,3n}$/+, *Fgf18*$^{+/-}$ or *Fgf17*$^{-/-}$, *Fgf8*$^{\Delta 2,3n}$/+ *Fgf18*$^{-/-}$ embryos may survive long enough to address this issue. There is a strong possibility that the defect in MHB development of these compound mutant mice may occur at stages prior to E11.5. Because the data presented here suggests that FGF signaling no longer regulates the expression of *En2, Wnt1, Pax5* and *Otx2* at E12.5, mouse mutants lacking alleles of *Fgf8, Fgf17* and *Fgf18* with deficits earlier in development will help to identify the stage between E9.5 and E12.5, where FGF signaling shifts from a role as an organizer to that of a growth and differentiation factor.

Regulation of neuronal differentiation in the vermis

The polarized progression of cerebellar differentiation was reported almost 15 years ago (Altman and Bayer, 1985). Unlike the extensive genetic studies on cerebellar patterning, the factors that control cerebellar growth and differentiation are largely unknown. One mystery, not explained by current models, is why differentiation in the vermis anlage proceeds in a caudolateral-to-rostromedial direction whereas differentiation in the cerebellar hemisphere anlage proceeds in a rostromedial to caudolateral direction. Here we have shown that prematurely decreasing and subsequently terminating FGF signaling in the vermis anlage accelerates the progression of Purkinje cell differentiation. We therefore propose that FGF8 and FGF17 normally function to inhibit differentiation in the vermis primordium. Such an inhibitory effect may be directly associated with the ability of FGF to maintain the precursor cell pool in an undifferentiated proliferating state, as demonstrated here and in other in vitro studies (Gritti et al., 1996; Johe et al., 1996), where FGF has been identified as a growth factor for CNS stem cells. Our observations suggest a model in which the polarized progression of differentiation in the vermis anlage may be achieved in part by the gradual decrease in *Fgf* expression and the gradual narrowing of the expression domains of *Fgf8, Fgf17* and *Fgf18* from E11.5 to E14.5. As a result of these dynamic changes in *Fgf* expression, precursor cells in the caudal part of the cerebellar primordium would first be released from FGF inhibition and subsequently allowed to differentiate, before those at the rostral end of the primordium where *Fgf* expression persists until E15.5 (Fig. 10). In addition, the polarized differentiation may also be facilitated by a previously reported, rostral-to-caudal, movement of isthmic cells (Hallonet and Le Douarin, 1993), which could push the precursor cells away from the field of FGF expression.

How many FGFs does it take to make a cerebellum?

In addition to *Fgf8, Fgf17* and *Fgf18, Fgf15* is also expressed in the developing cerebellum (McWhirter et al., 1997 and data not shown). Unlike *Fgf8, Fgf17* and *Fgf18, Fgf15* is expressed in the anlage of the cerebellar hemispheres at E9.5-E10.5, and later is more restricted to the caudal part of the cerebellar hemispheres. Because the differentiation of the cerebellar hemisphere proceeds in a rostral-to-caudal direction, opposite to that in the vermis (Altman and Bayer, 1997), we hypothesize that the onset of differentiation in the cerebellar hemisphere and in the vermis are independently regulated by two different FGF gradients mediated by the *Fgf8* family medially and by *Fgf15* laterally.

Consistent with the expression of *Fgf15* during cerebellar development, it is tempting to speculate that *Fgf15* may also regulate the growth of the cerebellar hemispheres. This hypothesis helps to explain why tissue loss in mice lacking alleles of *Fgf8* and *Fgf17* is restricted to the vermis. Intriguingly, *Fgf19*, is most closely related to *Fgf15* (Nishimura et al., 1999) and preliminary data suggests that *Fgf19* is also expressed in the developing CNS. It will therefore be interesting to see if *Fgf19* is also expressed in the developing cerebellar hemisphere. Interestingly, the subfamily of *Fgf15* and *Fgf19* is phylogenetically more related to the *Fgf8* subfamily than to other subfamilies of *Fgf*s (data not shown) and is therefore likely to share similar receptor specificity towards FGFRs expressed in the neuroepithelial primordium. Phylogenetic analysis (Coulier et al., 1997) suggests that the FGF family has grown by gene duplication events throughout evolution, which may have contributed to the disproportional increase in cerebellar size seen in higher animals.

This work was supported by NIH grant CA60673 and a grant from the American Heart Association. We are grateful to E. Spinaio and X. Hua for their technical help, G. Martin and E. Meyers for generously providing *Fgf8*$^{\Delta 2,3n}$/+ mice and A. P. McMahon, A. L. Joyner and P. Gruss for providing in situ hybridization probes. We thank R. Kopan, I. Boime and R. Cagan for critically reading this manuscript.

REFERENCES

Altman, J. and Bayer, S. A. (1985). Embryonic development of the rat cerebellum. III. Regional differences in the time of origin, migration, and settling of Purkinje cells. *J. Comp. Neurol.* 231, 42-65.

Altman, J. and Bayer, S. A. (1997). *Development of the Cerebellar System: In Relation to its Evolution, Structure and Functions*. New York: CRC press.

Alvarez Otero, R., Sotelo, C. and Alvarado-Mallart, R. M. (1993). Chick/quail chimeras with partial cerebellar grafts: an analysis of the origin and migration of cerebellar cells. *J. Comp. Neurol.* **333**, 597-615.

Bally-Cuif, L., Alvarado-Mallart, R. M., Darnell, D. K. and Wassef, M. (1992). Relationship between *Wnt-1* and *En-2* expression domains during early development of normal and ectopic met-mesencephalon. *Development* **115**, 999-1009.

Brodal, P. (1998). *The Central Nervous System: Structure and Function*. Oxford: Oxford University Press.

Chisaka, O. and Capecchi, M. R. (1991). Regionally restricted development defects resulting from targeted disruption of the mouse homeobox gene *hox-1.5*. *Nature* **350**, 473-479.

Coulier, F., Pontarotti, P., Roubin, R., Hartung, H., Goldfarb, M. and Birnbaum, D. (1997). Of worms and men: an evolutionary perspective on the fibroblast growth factor (FGF) and FGF receptor families. *J. Mol. Evol.* **44**, 43-56.

Crossley, P. H., Martinez, S. and Martin, G. R. (1996). Midbrain development induced by FGF8 in the chick embryo. *Nature* **380**, 66-68.

Gardner, C. A. and Barald, K. F. (1991). The cellular environment controls the expression of engrailed-like protein in the cranial neuroepithelium of quail-chick chimeric embryos. *Development* **113**, 1037-48.

Gritti, A., Parati, E. A., Cova, L., Frolichsthal, P., Galli, R., Wanke, E., Faravelli, L., et al. (1996). Multipotential stem cells from the adult mouse brain proliferate and self-renew in response to basic fibroblast growth factor. *J. Neurosci.* **16**, 1091-100.

Hallonet, M. and Alvaradomallart, R. M. (1997). The chick/quail chimeric system – a model for early cerebellar development. *Perspec. Dev. Neurol.* **5**, 17-31.

Hallonet, M. E. and Le Douarin, N. M. (1993). Tracing neuroepithelial cells of the mesencephalic and metencephalic alar plates during cerebellar ontogeny in quail-chick chimaeras. *Eur. J. Neurosci.* **5**, 1145-55.

Hatten, M. E. and Heintz, N. (1995). Mechanisms of neural patterning and specification in the developing cerebellum. *Annul. Rev. Neurosci.* **18**, 385-408.

Hogan, B. L. M. and Yingling, J. M. (1998). Epithelial/Mesenchymal

Interactions and Branching Morphogenesis of the Lung. *Curr. Opin. Genet. Devel.* **8**, 481-486.

Itasaki, N., Ichijo, H., Hama, C., Matsuno, T. and Nakamura, H. (1991). Establishment of rostrocaudal polarity in tectal primordium: engrailed expression and subsequent tectal polarity. *Development* **113**, 1133-44.

Johe, K. K., Hazel, T. G., Muller, T., Dugich-Djordjevic, M. M. and McKay, R. D. (1996). Single factors direct the differentiation of stem cells from the fetal and adult central nervous system. *Genes Dev.* **10**, 3129-40.

Joyner, A. L. (1996). *Engrailed*, *Wnt* and *Pax* genes regulate midbrain–hindbrain development. *Trends Genet.* **12**, 15-20.

Lee, S. M., Danielian, P. S., Fritzsch, B. and McMahon, A. P. (1997). Evidence that FGF8 signalling from the midbrain-hindbrain junction regulates growth and polarity in the developing midbrain. *Development* **124**, 959-969.

Lewandoski, M., Wassarman, K. M. and Martin, G. R. (1997). Zp3-cre, a transgenic mouse line for the activation or inactivation of loxP-flanked target genes specifically in the female germ line. *Curr. Biol.* **7**, 148-51.

Liu, A., Losos, K. and Joyner, A. L. (1999). FGF8 can activate Gbx2 and transform regions of the rostral mouse brain into a hindbrain fate. *Development* **126**, 4827-4838.

Marin, F. and Puelles, L. (1995). Morphological fate of rhombomeres in quail/chick chimeras: a segmental analysis of hindbrain nuclei. *Eur. J. Neurosci.* **7**, 1714-38.

Martinez, S., Crossley, P. H., Cobos, I., Rubenstein, J. L. and Martin, G. R. (1999). FGF8 induces formation of an ectopic isthmic organizer and isthmocerebellar development via a repressive effect on Otx2 expression. *Development* **126**, 1189-200.

Martinez, S., Wassef, M. and Alvarado-Mallart, R. M. (1991). Induction of a mesencephalic phenotype in the 2-day-old chick prosencephalon is preceded by the early expression of the homeobox gene en. *Neuron* **6**, 971-81.

Maruoka, Y., Ohbayashi, N., Hoshikawa, M., Itoh, N., Hogan, B. L. M. and Furuta, Y. (1998). Comparison of the expression of three highly related genes, *Fgf8*, *Fgf17* and *Fgf18*, in the mouse embryo. *Mech. Dev.* **74**, 175-177.

McKeehan, W. L., Wang, F. and Kan, M. (1998). The heparan sulfate-fibroblast growth factor family: diversity of structure and function. *Prog. Nucleic Acid Res. Mol. Biol.* **59**, 135-176.

McMahon, A. P., Joyner, A. L., Bradley, A. and McMahon, J. A. (1992). The midbrain-hindbrain phenotype of *Wnt-1*$^{-}$*/Wnt-1*$^{-}$ mice results from stepwise deletion of engrailed-expressing cells by 9.5 days postcoitum. *Cell* **69**, 581-95.

McWhirter, J. R., Goulding, M., Weiner, J. A., Chun, J. and Murre, C. (1997). A novel fibroblast growth factor gene expressed in the developing nervous system is a downstream target of the chimeric homeodomain oncoprotein E2A-Pbx1. *Development* **124**, 3221-3232.

Meyers, E. N., Lewandoski, M. and Martin, G. R. (1998). An *Fgf8* mutant allelic series generated by Cre- and Flp-mediated recombination. *Nat. Genet.* **18**, 136-141.

Naski, M. C., Colvin, J. S., Coffin, J. D. and Ornitz, D. M. (1998). Repression of hedgehog signaling and BMP4 expression by fibroblast growth factor receptor 3 in growth plate cartilage of transgenic mice. *Development* **12**5, 4977-4988.

Naski, M. C. and Ornitz, D. M. (1998). FGF signaling in skeletal development. *Front. Biosci.* **3**, D781-794.

Nishimura, T., Utsunomiya, Y., Hoshikawa, M., Ohuchi, H. and Itoh, N. (1999). Structure and expression of a novel human FGF, FGF-19, expressed in the fetal brain. *Biochem. Biophys. Acta* **1444**, 148-151.

Ornitz, D. M., Xu, J., Colvin, J. S., McEwen, D. G., MacArthur, C. A., Coulier, F., Gao, G., et al. (1996). Receptor specificity of the fibroblast growth factor family. *J. Biol. Chem.* **271**, 15292-15297.

Reifers, F., Bohli, H., Walsh, E. C., Crossley, P. H., Stainier, D. Y. and Brand, M. (1998). *Fgf8* is mutated in zebrafish *acerebellar* (*ace*) mutants and is required for maintenance of midbrain-hindbrain boundary development and somitogenesis. *Development* **125**, 2381-95.

Schwarz, M., Alvarez-Bolado, G., Dressler, G., Urbanek, P., Busslinger, M. and Gruss, P. (1999). *Pax2/5* and *Pax6* subdivide the early neural tube into three domains. *Mech. Dev.* **82**, 29-39.

Shamim, H., Mahmood, R., Logan, C., Doherty, P., Lumsden, A. and Mason, I. (1999). Sequential roles for *Fgf4*, *En1* and *Fgf8* in specification and regionalisation of the midbrain. *Development* **126**, 945-59.

Sheikh, H. and Mason, I. (1996). Polarising activity of FGF-8 in the avian midbrain. *Int. J. Dev. Biol.* **Supplement**, 117S-118S.

Szebenyi, G. and Fallon, J. F. (1999). Fibroblast growth factors as multifunctional signaling factors. *Int. Rev. Cyt.* **185**, 45-106.

Tybulewicz, V. L. J., Crawford, C. E., Jackson, P. K., Bronson, R. T. and Mulligan, R. C. (1991). Neonatal lethality and lymphopenia in mice with a homozygous disruption of the *c-abl* proto-oncogene. *Cell* **65**, 1153-1163.

Victor, M., Adams, R. D. and Mancall, E. L. (1959). A restricted form of cerebellar cortical degeneration occurring in alcoholic patients. *Arch. Neurol.* **1**, 579-699.

Xu, J., Lawshe, A., MacArthur, C. A. and Ornitz, D. M. (1999). Genomic structure, mapping, activity and expression of fibroblast growth factor 17. *Mech. Dev.* **83**, 165-78.

Yuasa, S., Kawamura, K., Ono, K., Yamakuni, T. and Takahashi, Y. (1991). Development and migration of Purkinje cells in the mouse cerebellar primordium. *Anat. Embryol.* **184**, 195-212.